Formation and Characterization of Filamentary Current Paths in HfO_2-Based Resistive Switching Structures

F. Palumbo, *Member, IEEE*, E. Miranda, *Senior Member, IEEE*, G. Ghibaudo, and V. Jousseaume

***Abstract*—In this letter, the progressive nature of the forming process step in HfO_2-based resistive switching structures is investigated. Contrary to what happens with ramped or pulsed voltage stresses, current-driven degradation experiments shed light on the formation dynamics of the filamentary path across the oxide layer. The resulting voltage–current characteristics are interpreted in terms of electron transport through a mesoscopic constriction with adiabatic shape. The voltage decrease during the forming process is ascribed to a relaxation of the electron wavefunction confinement effect. The role of the compliance level on the leakage current magnitude is also discussed within this framework.**

***Index Terms*—Dielectric breakdown, resistive switching (RS).**

I. Introduction

THE resistive switching (RS) phenomenon in metal–insulator–metal (MIM) structures is currently attracting a lot of attention from academia and industry due to its potential applicability for nonvolatile memory devices [1], [2]. HfO_2 is particularly important as a switching material mainly because of its compatibility with standard complementary metal–oxide–semiconductor technology. The devices often require an initial forming step, which, in case of a voltage ramp, is associated with a sudden current increase. On the contrary, as shown in this letter, the use of current ramped stress allows to capture the details of the forming dynamics, which is eventually determined by the interplay between lateral expansion of the filamentary path and voltage reduction, the latter being a key parameter for the degradation rate of dielectric films [3]. Remarkably, this evolutionary behavior closely resembles the so-called progressive dielectric breakdown of ultrathin SiO_2 layers in MOS structures, in which the lateral size of the leakage path increases with time as well [4]. Since the current flow in this latest regime has been demonstrated to be highly localized and the Landauer theory has proven to be useful for modeling, the conduction characteristics of our MIM devices will be analyzed using the same concepts [5]. Here, how this theory not only provides a consistent explanation for the voltage-currrent (V–I) characteristics during stress but also provides for the connection between current magnitude and size of the filamentary path will be shown.

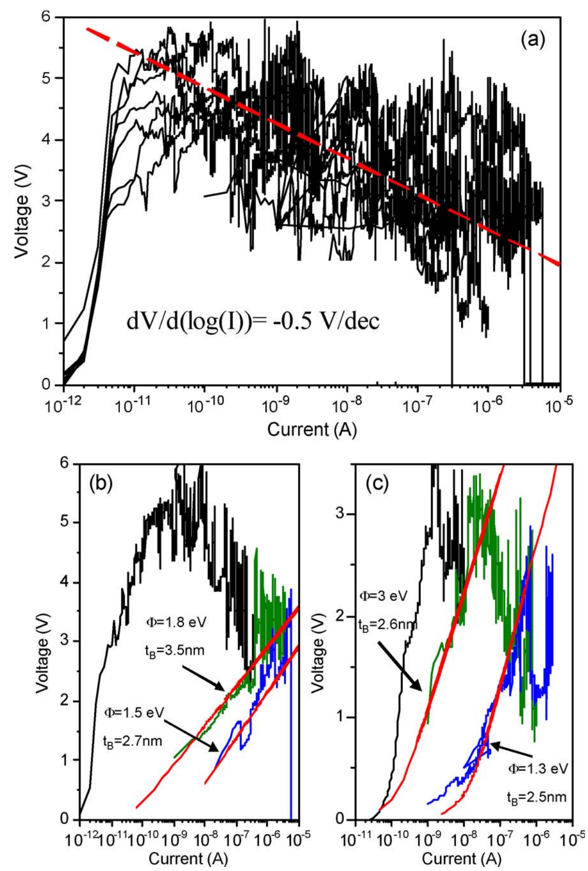

Fig. 1. (a) Typical V–I characteristics measured on our Pt/HfO_2/Pt structures. Several curves are superimposed in order to show the common trend of the forming event. (b) and (c) are two particular cases in which the current is stopped at some prescribed values and resumed starting from a lower initial value. The different colors (black, green, and blue) correspond to consecutive V–I curves. The red solid lines are fittings to the experimental data using (1).

Manuscript received March 4, 2012; accepted March 31, 2012. Date of publication May 4, 2012; date of current version June 22, 2012. This work was supported in part by the Consejo Nacional de Investigaciones Científicas y Técnicas (CONICET), Argentina, under Grant PIP-1063, by the International Centre of Theoretical Physics, Italy, by the Ministry of Science and Innovation under Grant TEC09-09350, and by the DURSI of the Generalitat de Catalunya, Spain, under Grant 2009SGR783. The review of this letter was arranged by Editor M. Jurczak.

F. Palumbo is with the Consejo Nacional de Investigaciones Científicas y Técnicas–Comision Nacional de Energia Atomica (CONICET-CNEA), 1650 Buenos Aires, Argentina (e-mail: palumbo@cnea.gov.ar).

E. Miranda is with the Departament d'Enginyeria Electrònica, Universitat Autònoma de Barcelona, 08193 Barcelona, Spain.

G. Ghibaudo is with IMEP-LAHC-MINATEC, 38054, Grenoble Cedex 9, France.

V. Jousseaume is with CEA-LETI-MINATEC, 38054, Grenoble Cedex 9, France.

Color versions of one or more of the figures in this letter are available online at http://ieeexplore.ieee.org.

Digital Object Identifier 10.1109/LED.2012.2194689

0741-3106/$31.00 © 2012 IEEE

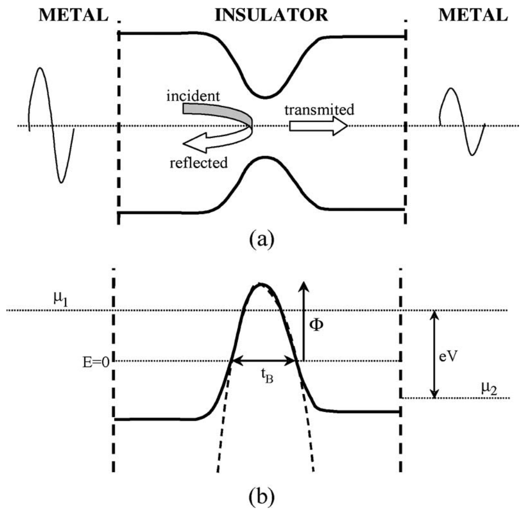

Fig. 2. (a) Schematic diagram of the tubelike constriction associated with RS. (b) Potential barrier is a consequence of the tighter confinement effect at the constriction's bottleneck. Φ is the barrier height, and t_B is the barrier width at the reference energy level $E = 0$. $\mu_1 - \mu_2 = eV$, where μ_1 and μ_2 are the quasi-Fermi levels deep inside the reservoirs.

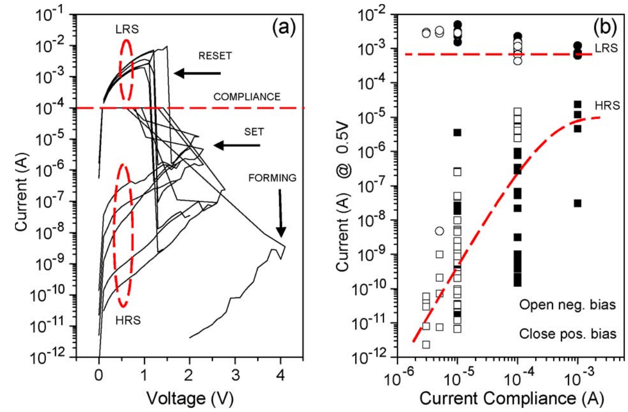

Fig. 3. Typical electrical characteristics of our MIM structures. (a) Consecutive curves showing the transition between LRS and HRS. A current compliance of 100 μA is used. (b) Current measured at low voltages (±0.5 V) for LRS and HRS as a function of the compliance level.

II. Sample Description and Forming Process

The devices used in this letter are $Pt/HfO_2/Pt$ structures with an area of 5×10^{-9} cm^2. The oxide layer (10 nm thick) was grown by atomic layer deposition. Further details about the structures under investigation can be found in [2].

Fig. 1(a) shows V–I measurements performed on different devices in a wide range of currents (nearly seven orders of magnitude). The onset of breakdown is detected by a noisy behavior followed by a voltage reduction trend with slope $dV/d\log(I) = -0.5$ V/dec. In Fig. 1(b) and (c), the current is stopped at some prescribed values and subsequently resumed starting from a lower initial current value. In all the cases, an abrupt voltage drop finally points out the completion of the filamentary path. The negative differential resistance region starting around 10^{-9}–10^{-8} A is a clear indication that a gradual and irreversible modification of the transmission properties of the leakage path is taking place during stress. The large voltage fluctuations occurring during this stage may also be regarded as the signature of atomic rearrangements in a low-dimensionality conducting system. In terms of thin oxide reliability, this noisy region corresponds to the so-called soft breakdown failure mode [3].

III. Analysis of the Conduction Characteristics

In this section, we will show that the V–I characteristics reported in Fig. 1 can be interpreted in terms of ballistic electron transport through a mesoscopic constriction with adiabatic shape [see Fig. 2(a)]. Of course, this oversimplified analysis rules out any possibility of modeling the voltage fluctuations, and only the main trend will be considered. According to the Landauer theory, the current that flows through a filamentary structure is dictated by the size of the constriction's bottleneck and the contact resistances with the two metal reservoirs [6]. Fig. 2(b) shows the energy profile along the constriction corresponding to the high-resistance state (HRS). This is the state just at the outset of the voltage fluctuations in Fig. 1. For the sake of simplicity, it is assumed that the applied bias mainly drops at the two ends of the constriction. The potential barrier is not material related but corresponds to the bottom of the first quantized subband associated with the lateral confinement of the electron wavefunction. Assuming an inverted parabolic barrier approximation, the V–I characteristic obtained from the finite-bias Landauer approach reads [5]

$$V = \frac{2}{\alpha e}\sinh^{-1}\left[\frac{h\alpha \operatorname{sinc}(\pi k T\alpha)}{4e\exp(-\alpha\Phi)}\right] \tag{1}$$

where $\alpha = t_B h^{-1}\pi^2\sqrt{2m^*/\Phi}$ with Φ denoting the barrier height, t_B denoting the barrier width at $E = 0$, m^* denoting the electron effective mass in the constriction ($m^* = 0.11$ m[7]), $T = 300$ K denoting the temperature, h denoting the Planck constant, k denoting the Boltzmann constant, and m and e denoting the electron mass and charge, respectively. Fig. 1(b) and (c) shows fitting results using (1). Barrier heights of only a few electronvolts and barrier widths in the nanometer range are obtained, which is consistent with an atomic-sized constriction picture. An approximate value for the lateral size of the constriction (< 1 nm) can also be found from the first eigenvalue of a cylindrical well following the method reported in [5]. From (1), the voltage decrease with increasing current values can be ascribed to a reduction of Φ, to a reduction of t_B, or both, which can, in turn, be regarded as a consequence of the relaxation of the confinement effect (increase of the constriction's cross-sectional area). Notice that, the low-resistance state (LRS) for a monomode ballistic conductor can be achieved by considering $\alpha \to 0$ in (1), which corresponds to transmission probability equal to unity in the Landauer formula. This limit yields a linear I–V in agreement with the LRS experimental data. This is the state found immediately after the final voltage jump in Fig. 1.

In order to investigate the role of the electron confinement effect on the leakage current magnitude, different current compliance levels were used to limit the damage caused to the structure during the set operation. Fig. 3(a) shows typical RS behavior exhibited by our structures. After the initial forming step, consecutive I–V curves show unipolar transitions between HRS and LRS. The large variations observed in HRS

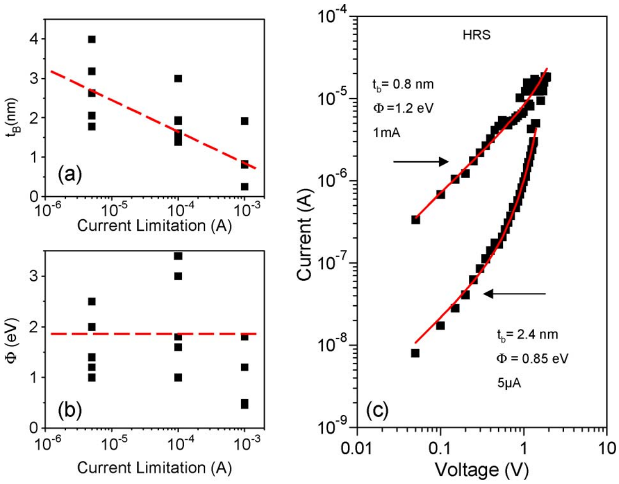

Fig. 4. (a) t_B as a function of the current limitation during the set operation. (b) Φ as a function of the current limitation. All values were obtained from fitting results using (1). (c) HRS I–V characteristics obtained with different current limitations. The solid lines correspond to model results, and the symbols are experimental data.

are consistent with the voltage fluctuations shown in Fig. 1. Fig. 3(b) shows the effects of varying the compliance level on the current magnitude (I at 0.5 V). Notice the strong dependence of HRS with compliance. On the contrary, LRS is practically unaffected by this limitation. This behavior is compatible with our vision of RS: While the HRS current depends exponentially on Φ and $t_B(1)$, i.e., on the particular features of the constriction's bottleneck, the LRS current is almost insensitive to these parameters (it varies within the same order of magnitude) because the limiting factors are now mainly the contact resistances. Moreover, to directly unveil the role played by the compliance level on the constriction's parameters, different sets of HRS I–V curves were analyzed using (1). The fitting parameters Φ and t_B are plotted in Fig. 4(a) and (b) and were extracted from curves similar to those shown in Fig. 4(c). Notice that, although no clear trend is observed for Φ, t_B indeed decreases as the current compliance increases, i.e., as the damage caused to the filamentary structure during the set operation increases. This seems to indicate that larger damages or higher currents are associated with a closer location of the atoms or vacancies that form the bottleneck of the conducting bridge rather than to an increment of its minimum cross section. A similar relationship for a linear chain of defects in broken down SiO_2 films has been reported in [7] using Harrison's method for atomic orbitals.

IV. Conclusion

Current-driven stress experiments have revealed the nature of the forming process in HfO_2 layers, a behavior that closely resembles the progressive dielectric breakdown of ultrathin SiO_2 layers in MOS structures. As in this latter case, the transition between the HRS and LRS is ascribed to a gradual change of the electron wavefunction confinement potential, which, in turn, is linked to the physical size of the filamentary path. This change can be originated by the movement of charged species or defects during the set sweep or by Joule heating effects in the case of the reset process.

References

[1] R. Waser and M. Aono, "Nanoionics-based resistive switching memories," *Nat. Mater.*, vol. 6, no. 11, pp. 840–883, Nov. 2007.

[2] V. Jousseaume, A. Fantini, J. Nodin, C. Guedj, A. Persico, J. Buckley, S. Tirano, P. Lorenzi, R. Vignon, H. Feldis, S. Minoret, H. Grampeix, A. Roule, S. Favier, E. Martinez, P. Calka, N. Rochat, G. Auvert, J. Barnes, P. Gonon, C. Vallée, L. Perniola, and B. De Salvo, "Comparative study of non-polar switching behaviors of NiO- and HfO_2-based oxide resistive-RAM," in *Proc. IEEE IMW*, Seoul, South Korea, May 16–19, 2010, pp. 1–4.

[3] S. Lombardo, J. H. Stathis, B. P. Linder, K. L. Pey, F. Palumbo, and C. H. Tung, "Dielectric breakdown mechanisms in gate oxides," *J. Appl. Phys.*, vol. 98, no. 12, pp. 121–301, Dec. 2005.

[4] E. Miranda, "Mesoscopic approach to progressive breakdown in ultrathin SiO_2 layers," *Appl. Phys. Lett.*, vol. 91, no. 5, p. 053 502, Jul. 2007.

[5] E. Miranda, C. Walczyk, C. Wenger, and T. Schroeder, "Model for the resistive switching effect in HfO_2 MIM structures based on the transmission properties of narrow constrictions," *IEEE Electron Devices Lett.*, vol. 31, no. 6, pp. 609–611, Jun. 2010.

[6] S. Datta, *Electronic Transport in Mesoscopic Systems*. Cambridge, U.K.: Cambridge Univ. Press, 1997.

[7] M. Xu and C. Tan, "Defect band structure investigation of postbreakdown SiO_2," *Appl. Phys. Lett.*, vol. 92, no. 8, p. 082 905, Feb. 2008.